J. Cardiovasc. Dev. Dis. **2014**, *2*, 163-176; doi:10.3390/jcdd1020163

OPEN ACCESS

Journal of
Cardiovascular
Development and Disease

ISSN 2308-3425
www.mdpi.com/journal/jcdd

Article

Sox9- and Scleraxis-Cre Lineage Fate Mapping in Aortic and Mitral Valve Structures

Blair F. Austin [1], Yuki Yoshimoto [2], Chisa Shukunami [2] and Joy Lincoln [1,3,*]

[1] Center for Cardiovascular and Pulmonary Research and The Heart Center at Nationwide Children's Hospital Research Institute, 575 Children's Drive, Research Building III, WB4239, Columbus, OH 43215, USA; E-Mail: blair.austin@nationwidechildrens.org

[2] Department of Molecular Biology and Biochemistry, Division of Basic Life Sciences, Institute of Biomedical & Health Sciences, Hiroshima University, Hiroshima 734-8553, Japan; E-Mails: yoshimoto@hiroshima-u.ac.jp (Y.Y.); shukunam@hiroshima-u.ac.jp (C.S.)

[3] Department of Pediatrics, The Ohio State University, Columbus, OH 43205, USA

* Author to whom correspondence should be addressed; E-Mail: joy.lincoln@nationwidechildrens.org; Tel.: +1-614-355-5752; Fax: +1-614-355-5752.

Received: 26 August 2014; in revised form: 16 September 2014 / Accepted: 17 September 2014 / Published: 23 September 2014

Abstract: Heart valves are complex structures composed of a heterogeneous population of valve interstitial cells (VICs), an overlying endothelium and highly organized layers of extracellular matrix. Alterations in valve homeostasis are characteristic of dysfunction and disease, however the mechanisms that initiate and promote valve pathology are poorly understood. Advancements have been largely hindered by the limited availability of tools for gene targeting in heart valve structures during embryogenesis and after birth. We have previously shown that the transcription factors Sox9 and Scleraxis (Scx) are required for heart valve formation and in this study we describe the recombination patterns of Sox9- and Scx-Cre lines at differential time points in aortic and mitral valve structures. In *ScxCre; ROSA26GFP* mice, recombination is undetected in valve endothelial cells (VECs) and low in VICs during embryogenesis. However, recombination increases in VICs from post natal stages and by 4 weeks side-specific patterns are observed. Using the inducible *Sox9CreERT2* system, we observe recombination in VECs and VICs in the embryo, and high levels are maintained through post natal and juvenile stages. These Cre-drivers provide the field with new tools for gene targeting in valve cell lineages during differential stages of embryonic and post natal maturation and maintenance.

Keywords: heart valve; endothelial; interstitial; Sox9; Scleraxis; aortic; mitral

1. Introduction

In the heart, there are two sets of valves: the atrioventricular (AV) consisting of the mitral and tricuspid that separate the atria from the ventricles on the left and right sides respectively; and the semilunar (SL), which includes the aortic and pulmonic valves that separate the ventricles from the great arteries [1]. Each valve set is composed of leaflets (AV) or cusps (SL) and supporting structures. In the AV position, external chordae tendineae attach the underside of the leaflets to the papillary muscles within the ventricular chambers, while SL valves lack external support but develop an internal substitute within the cusps [2]. Despite the anatomical differences, the function of the AV and SL valves are similar and serve to maintain unidirectional blood flow through the heart during the cardiac cycle by opening and closing during diastole and systole, respectively. This is largely achieved by the biomechanical properties provided by organized layers of extracellular matrices (ECM) including collagens, proteoglycans and elastins that form the fibrosa, spongiosa and ventricularis (AV)/atrialis (SL), respectively [2]. Homeostasis of the valve ECM is maintained by valve interstitial cells (VICs), which reside within the mature valve leaflets as quiescent fibroblast-like cells in the absence of disease [3]. In addition to this cell population, a layer of valve endothelial cells (VECs) surround the leaflets and serve to sense changes in the hemodynamic environment and molecularly communicate with underlying VICs to regulate their behavior [1,4–7]. Together, integration between the ECM and cellular components of the valve structure is essential for normal valve structure and function as alterations in ECM organization or cell function are associated with valve dysfunction.

Formation of heart valve structures is initiated during embryogenesis with development of endocardial cushions in the developing AV canal and outflow tract regions. These ECM-rich structures form as a result of endothelial-to-mesenchyme transformation (EMT) beginning around E9.5 in the mouse [8,9]. As development progresses the cushions expand as a result of mesenchyme cell proliferation and further elongate to form valve primordia by E14.5 [8]. As valvulogenesis continues, cell proliferation decreases and precursor cells lose expression of mesenchymal markers and function as activated myofibroblast-like VICs including secretion of ECM components that form the stratified layers after birth [10].

The development of the *Cre/LoxP* system has allowed for elegant studies to define the cell lineages that contribute to the valve structures, and determine their origin and fate. These approaches rely on the use of cell- and tissue-specific *Cre* lines bred with *ROSA26* (*Gt(ROSA)26Sor*) reporter mice that express *LacZ, GFP* or *eYFP* in *Cre*-positive lineages following recombination of the *loxP* sites [11]. Utilization of the *Tie2-cre* transgene [12] has allowed for candidate gene targeting in endothelial, and endothelial-derived cells within the endocardial cushion [8,9]. The limitations of this transgene for valve studies is that it is not restricted to valve endothelial cells (VECs), but expressed in this cell lineage throughout the developing embryo in addition to bone marrow-derived cells. Furthermore, the widespread recombination pattern of *Tie2-cre* in VECs, and VICs derived through EMT prevent endothelial cell-specific studies during post EMT stages. To address this limitation, Forde *et al.* published an inducible *Tie2-Cre* transgene containing an estrogen receptor fusion protein ER (T2) that allows for

temporal recombination in endothelial cells following exposure to an estrogen antagonist, commonly tamoxifen [13]. Using this approach, gene targeting in VECs (and other endothelial cells), but not VICs can be performed once EMT is complete. In addition to *Tie2-creER (T2)*, Robson *et al.* [14] reported temporal recombination of *Cdh5(PAC)-ERT2* in VECs. However, similar to the *Tie2* models, *Cdh5* is not exclusive to endothelial cells of the valves. More recently, others have identified a 250 bp enhancer region with the first intron of mouse *Nfatc1* [15] and subsequently generated a *Cre* line [16] that recombines predominantly in VECs, with limited recombination in the endocardium. The advantage of this model is that VECs expressing the 250 bp enhancer do not undergo EMT and therefore, although this model is not inducible, recombination does not occur in endothelial-derived VICs making it an attractive system for studying VEC biology.

In addition to the generation of endothelial-specific *Cre* drivers, the field is emerging with several *Cres* that target non-endothelial cells of the valves. This includes the *Wnt1-cre* transgene that recombines in neural crest-derived cells predominant in outflow tract [17] and AV [18] cushions. Recombination of *Mef2c-cre* in second heart field-derived cells is also high in mesenchyme cells within the endocardial cushions [19,20]. Once endocardial cushion formation is complete, recombination of additional *Cre* drivers are observed in the valves including *Wt1-cre* labeled epicardially-derived cells within the parietal leaflets of the mitral and tricuspid valve [21–23]. Furthermore, *Col2a1-cre* [24] recombines in a small population of "sub-endothelial" VICs within the fibrosa layer of all valve sets from E15.5 [25]. More widespread *Cres* have also been utilized for heart valve studies including $Smad7^{Cre}$ active throughout the endocardial cushions as well as the endocardium and other tissues outside the heart including the jaw, limb buds and brain [26]. Reports have also shown that a 3.9 kb enhancer region of the fasciclin-containing adhesive glycoprotein *Periostin* (*Postn*) is expressed in mesenchyme, but not endothelial cells of the cushions; allowing for lineage-specific studies in embryonic valves [27–29]. However, these non-endothelial cell *Cres* are not inducible and therefore temporal studies of VIC biology after valve development have been hindered.

Our previous work has shown that transcription factors Sox9 and Scleraxis (Scx) are required for normal heart valve development. In mice, reduced *Sox9* function leads to premature calcification consistent with calcific aortic valve disease [25,30], while $Scx^{-/-}$ mice develop thickened valve leaflets associated with defects in ECM organization and VIC maturation [31]. While we have reported the endogenous expression patterns of Sox9 and Scx in the valves [25,30], recombination patterns of their respective *Cre* lines have not been characterized. *Scleraxis (Scx) Cre* mice were generated by Chisa Shukunami [32] and published work demonstrates recombination in tendons, ligaments, intervertebral discs, joints and cartilage, consistent with its published role in connective tissues of high mechanical demand [31–34]. Shukunami's group established two *ScxCre* lines expressing *Cre-recombinase* using a ~11 kb genomic region of the mouse *Scx* locus which recapitulates endogenous *Scx* seen in *ScxGFP* mice [32,35]. The two *ScxCre* transgenic lines have high (H) and low (L) copy numbers (*ScxCre-H*, *ScxCre-L)* and although the recombination patterns overlap, *ScxCre-H* activity is more widely distributed throughout the developing embryo [32]. In this study we describe the fate of *Scx*-derived cells in aortic and mitral valve structures at E15.5, post natal day (PND)12 and at 4 weeks of age using $Rosa26^{GFP}$ ($R26^{GFP}$) reporter mice. In addition, we utilize a tamoxifen inducible system to determine the contribution of $Sox9\text{-}creER^{T2}$ cells [36,37] to the left side valve structures at the same time points. Observations from these studies demonstrate the usefulness of these *Cre*-driver lines for temporal and spatial studies in embryonic and post natal heart valves.

2. Experimental Section

2.1. Generation of Mice

ScxCre-H and *ScxCre-L* mice were obtained from Dr. Chisa Shukunami [32], *Sox9CreER^{T2}* [36], and *ROSA26^{GFP}* mice were purchased from Jackson Labs (Stock numbers 018829 and 004077, respectively) and genotyped as described [32,36,38]. *Cre*-positive mice were bred with *ROSA26^{GFP} (R26^{GFP})* to generate double positive offspring. For *ScxCre* studies, *ScxCre-H;ROSA26^{GFP}* or *ScxCre-L:ROSA26^{GFP}* mice, and *Cre*-negative littermate controls were collected at E15.5, post natal day (PND) 12 and 4 weeks of age. In addition, tamoxifen (Sigma) was dissolved at 20 mg/mL in corn oil (Sigma) and administered intraperitoneally (IP) to pregnant *Sox9CreER^{T2}:ROSA26^{GFP}* females (2 mg per 40 g body weight) once a day from E14.5 and harvested 24 hours later at E15.5. Alternatively, PND10 pups and 4 week old mice were treated subcutaneously with 5 mg per 40 g body weight of tamoxifen once a day for 2 days before harvesting. All animal procedures were carried out in strict accordance with the recommendations in the Guide for the Care and Use of Laboratory Animals of the National Institutes of Health and approved by the IACUC Committee at Nationwide Children's Hospital Research Institute.

2.2. Histology and Immunohistochemistry

E15.5, PND12 and 4 week old whole hearts were harvested from *ScxCre-H:ROSA26^{GFP}*, *ScxCre-L:ROSA26^{GFP}* and *Sox9CreER^{T2}:ROSA26^{GFP}* mice and fixed in 4% paraformaldehyde/PBS overnight at 4 °C. Following fixation, fixed hearts were rinsed in 1 × Phosphate Buffer Saline (PBS) and processed for cryo embedding as described [30]. 6 μm frozen sections were then subject to fluorescent immunohistochemistry as described [39] using rabbit polyclonal α-GFP (Abcam ab290) at 1:1000 (50% block:PBS) and α-CD31 (Santa Cruz, C-20) at 1:1000. Antibodies were incubated on tissue sections overnight at 4 °C. Donkey α-rabbit-488 secondary (Invitrogen, Carlsbad, CA, USA) antibody was applied to the slides at 1:400 (PBS) for 1 hour at room temperature in the dark, followed by similar treatment with goat α-rat-568 to detect α-GFP and α-CD31, respectively. Stained tissue sections were mounted in Vectashield containing DAPI to detect nuclei. Images were captured using the Zeiss 710 confocal and Zen 2009 imaging software. Observations were made on at least n = 3 hearts from each *Cre*-driver line and respective controls.

3. Results and Discussion

The availability of heart valve specific *Cres* is limiting, and only recently have new *Cres* been identified that allow for more elegant temporal and spatial studies of heart valve cell lineages. While these *Cre* lines have advanced the field, there remains a demand for alternatives to further dissect the molecular and cellular mechanisms that underlie normal valve development and disease states. In this study, we characterize the recombination patterns of two *Cres* in aortic and mitral heart valve structures. *ScxCre-H* and *ScxCre-L* mice express *Cre-recombinase* using a ~11 kb genomic region of the mouse *Scx* locus which recapitulates endogenous *Scx* expression seen in *ScxGFP* mice [32,35]. The advantage of these differential *ScxCre* lines is that the level of activity (high or low) is controlled by copy number. *ScxCre* mice are not inducible and therefore using *ROSA26^{GFP}* we can detect the contribution of *Scx*-derived cells by GFP immunoreactivity from gastrulation until the time of harvest. At E15.5, *ScxCre-L*

recombination is observed in few VICs localized within the sub-endothelial lining of the aortic valve cusps (Figure 1A,B). In the mitral valve, few recombined VICs are observed and these are enriched within the distal tip of the leaflet. This infrequent *ScxCre* recombination is consistent with low levels of endogenous ScxGFP expression at this time [31]. Interestingly, *ScxCre-L* recombination was not observed in VECs at this embryonic time point. This current study did not examine *ScxCre-L* recombination events prior to E15.5, but based on our previous work showing endogenous Scx (-GFP) expression in a small population of mesenchymal valve precursor cells from E13.5 [31], we anticipate that *Cre* recombination occurs at low levels during early remodeling stages and is likely undetectable in endocardial cushions. In addition to the valves, low levels of *ScxCre-L* recombination are also observed within the developing myocardium (arrow, Figure 1E) consistent with its expression in cardiac fibroblasts [40], and the epicardium (arrow, Figure 1F).

At PND12, *ScxCre-L:R26*^{GFP} recombination in aortic, pulmonic, mitral and tricuspid valves remains low. However, a notable population of positive cells within the region of the aortic valve annulus is observed, and this cluster of cells remains labeled at 4 weeks of age (highlighted area, Figure 2A,B). At this time, GFP-positive VICs are also observed within the aortic valve cusp (arrow, Figure 2B), primarily associated with the fibrosa layer opposing blood flow (red arrow, Figure 2B). Similar to the aortic valve, few recombined *ScxCre-L* cells are observed in the mitral valve leaflets at PND12, however a large number of GFP-positive VICs are noted within the atrialis layer of the leaflet (arrow, Figure 2D) by 4 weeks. Consistent with embryonic observations, recombination of *ScxCre-L:R26*^{GFP} in VECs is rare (arrowhead, Figure 2A–D). Interestingly, *ScxCre-L:R26*^{GFP} GFP-positive cells are enriched within the fibrosa layer of the aortic valve cusps (Figure 2B), yet within the atrialis layer of the mitral valve leaflets (Figure 2D) at 4 weeks.

Compared to *ScxCre-L:R26*^{GFP}, recombination of *ScxCre-H:R26*^{GFP} is higher in VICs within the aortic valve cusps at PND12 as expected (arrow, Figure 2A,E), however expression is not observed within the annulus region (Figure 2E). Fewer recombined VICs are consistently observed within the distal tip region of both aortic and mitral valve leaflets of *ScxCre-H:R26*^{GFP} mice (Figure 2E–H), and similar to the *ScxCre-L:R26*^{GFP} line, recombination in CD31-positive VECs is negligible, if not undetected (arrowheads, Figure 2E–H). By 4 weeks of age, the contribution of *ScxCre-H:R26*^{GFP} cells to the mature aortic valve cusp appears less than at PND12 (Figure 2F), which may be attributed to the decreased survival of *Scx*-derived cells, or potential inefficiencies of *ScxCre-H* recombination by this stage. However in the mitral valve, the frequency of recombination in VICs is greater at 4 weeks compared to PND12. In *ScxCre-H* mice, recombination in VICs is observed throughout the leaflets at 4 weeks, and does not appear to be localized to a specific ECM layer. Together, these observations demonstrate that the *ScxCre* model is highly suited to studies targeting VIC sub-populations during later stages of development or early post natal maturation. In addition, these *Cre* lines can be controlled by copy number (*ScxCre-H versus ScxCre-L*), thereby avoiding high levels of recombination throughout the entire heterogeneous population of VICs. Based on the associated localization of *ScxCre-L* recombination along the atrialis of the mitral valve (Figure 2 D) and fibrosa of the aortic valve (Figure 2 B), it is considered that valve biomechanics may facilitate *ScxCre-L* activity, consistent with its role in tissues of high mechanical demand. In addition, as Scx is known to regulate expression of collagens and proteoglycans [40–42], it is likely that VIC-mediated Scx maintains ECM homeostasis within the mature valve.

Figure 1. *ScxCre-L* recombination in embryonic heart valve primorida structures. (**A**–**D**) Embryos were harvested from pregnant *ScxCre-L:R26*^{GFP} mice at E15.5 and immunohistochemistry was performed to detect GFP expression (Green) as an indicator of recombination, while CD31-(Red) identifies endothelial cells in aortic (**A**,**B**) and mitral (**C**,**D**) valves. (**B**) and (**D**) are high magnification images (40×) of the boxed areas shown in (**A**) and (**C**) at 10×, respectively. White arrows in (**B**) and (**D**) indicate valve endothelial cells, white concave arrow in (**B**) shows GFP-positive VICs within the sub-endothelial layer of the aortic valve. White concave arrows (**D**) show recombined valve interstitial cells within the distal tip of the developing valve primordia. (**E**–**F**) Arrows indicate few GFP-positive cells within the developing myocardium (**E**) and epicardium (**F**). DAPI (blue), indicates nuclei.

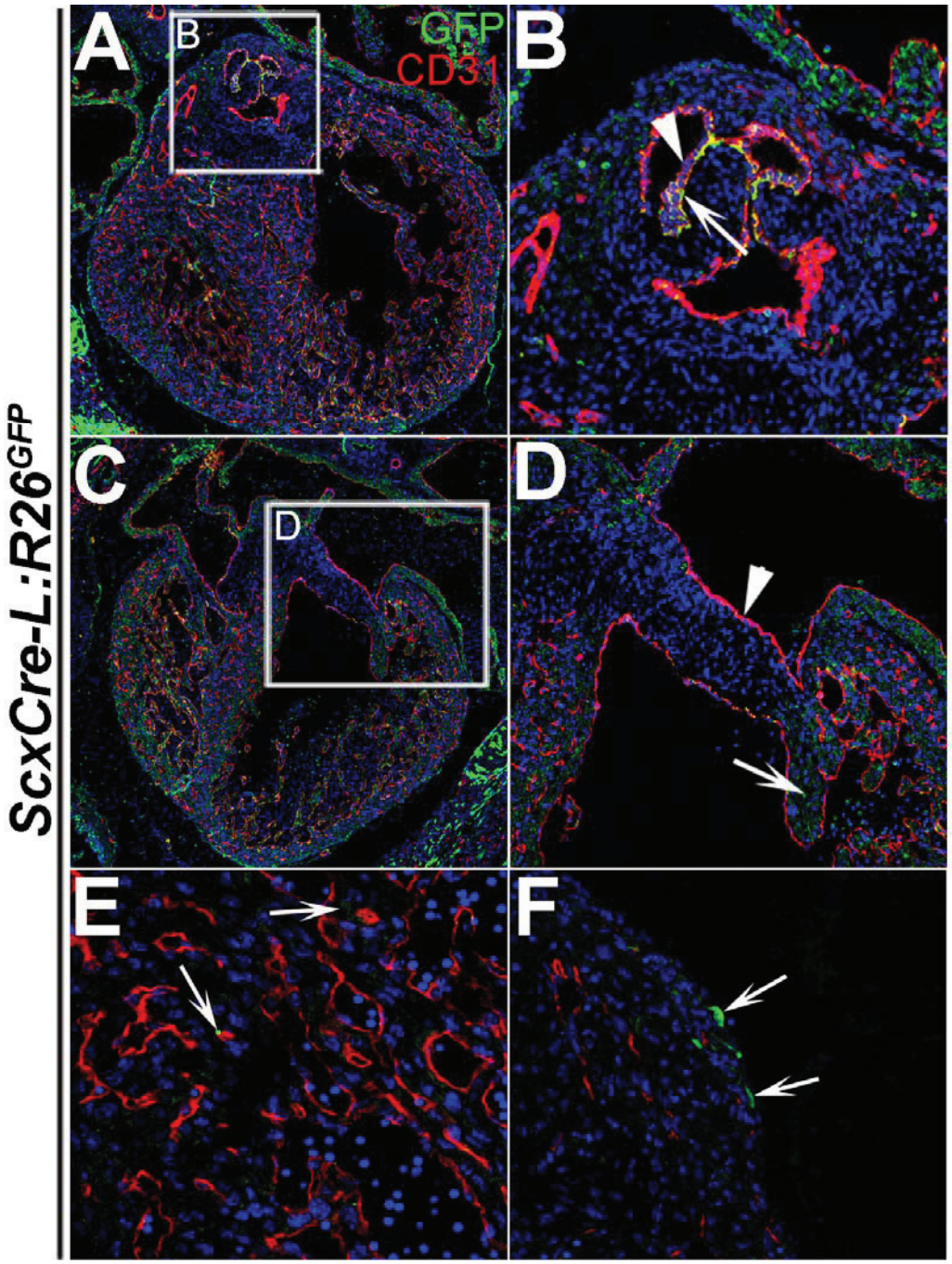

Figure 2. *ScxCre* recombination in post natal and juvenile heart valve structures. (**A**–**H**) Immunohistochemistry to detect GFP expression (Green) following *ScxCre:R26*^{GFP} recombination, and CD31- (Red) positive endothelial cells in aortic (**A**,**B**,**E**,**F**) and mitral (**C**,**D**,**G**,**H**) valves from PND12 (**A**,**C**,**E**,**G**) and 4 week (**B**,**D**,**F**,**H**) old *ScxCre-L:R26*^{GFP} (**A**–**D**) and *ScxCre-H:R26*^{GFP} (**E**–**H**) mice. Red arrows indicate blood flow direction. The highlighted regions in (**A**) and (**B**) indicate GFP-positive annular regions. White arrows indicate valve interstitial cells, and white arrows, valve endothelial cells. DAPI (blue), indicates nuclei.

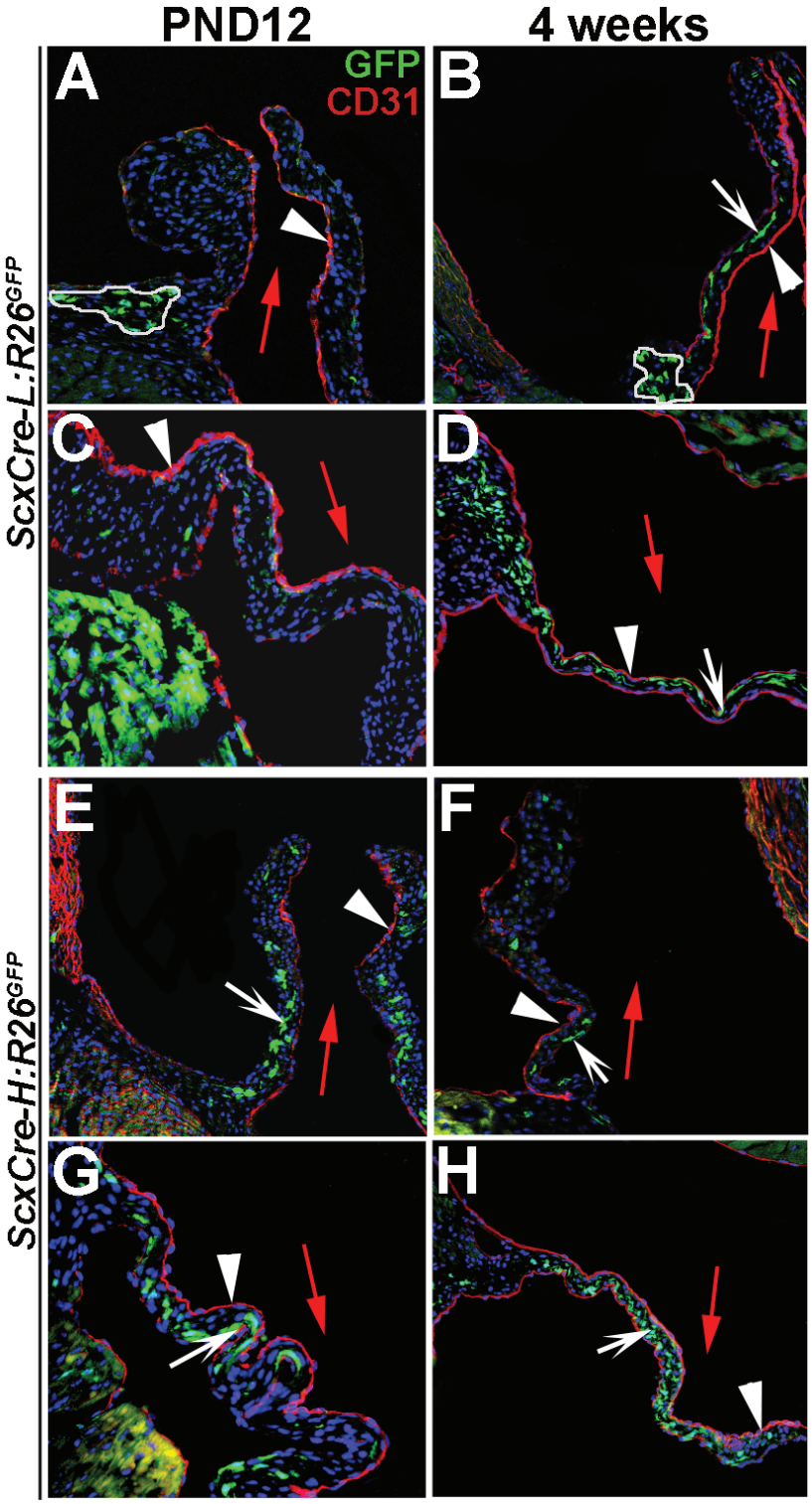

In contrast to the constitutively active *ScxCre* model, *Sox9CreER^{T2}:R26^{GFP}* mice contain an estrogen response element that for temporal activation following exposure to tamoxifen. In this study, pregnant *R26^{GFP}* females bred with *Sox9CreER^{T2}* males were treated once with tamoxifen by IP daily at E14.5, and harvested at E15.5. Therefore, recombination events shown in Figure 3 indicate *Sox9CreER^{T2}* activity within this 24-hour window. Few GFP-positive cells are observed within the pulmonic (data not shown) and aortic valve cusps at E15.5 (arrow, Figure 3B), however *Sox9CreER^{T2}* recombination is observed in a subset of VECs within the valve cusps (arrowhead, Figure 3B) and interstitial cells within the annular regions (red arrowhead, Figure 3B). In the tricuspid (data not shown) and mitral position, the number of VICs expressing GFP is much greater (arrow, Figure 3D) and low recombination is also detected in the developing myocardium (arrow, Figure 3E) and epicardium (arrow, Figure 3F). This level of recombination is comparable with endogenous Sox9 levels previously reported by our group, and consistent with its role in promoting expression of cartilaginous matrix proteins in valve primordial [25]. Further work is required to determine *Sox9CreER^{T2}* recombination prior to E15.5, however based on our previous studies showing that *Sox9* is required for proliferation of mesenchymal valve precursor cells [25], we anticipate that recombination would be high from as early as E9.5.

In addition to embryonic studies, *Sox9CreER^{T2}:R26^{GFP}* PND10 pups were exposed to tamoxifen for 48 hours and hearts were harvested at PND12. Similar to endogenous Sox9 expression studies [43], *Sox9CreER^{T2}* recombination remains low in the aortic valve cusp soon after birth (Figure 4A). However, at 4 weeks of age recombination is observed in a large population of VICs (concave arrow, Figure 4B) and VECs (arrowhead, Figure 4B) within the cusp. Notable recombination is reduced in the distal tip. In contrast to the aortic valve, recombination is high in VICs (concave arrow, Figure 4C) and VECs (arrowhead, Figure 4C) in the mitral valve at PND12 and this is reduced by 4 weeks of age (Figure 4D). We observe greater GFP expression levels in the parietal, compared to the septal leaflet of the mitral valve at PND12 (right, Figure 4C). Further studies are needed to investigate this further in both mitral and tricuspid valves, but this is interesting as Sox9 is expressed within epicardium and AV sulcus regions and these cell populations are known to contribute to the VIC population within the parietal leaflets [21]. Therefore, suggesting that the contribution of *Sox9*-derived cells is likely from multiple sources within the mitral valve leaflets. Together, these expression studies suggest that *Sox9CreER^{T2}:R26^{GFP}* mice demonstrate recombination in both VICs and VECs, however *Cre* activity is much lower in the aortic valve compared to the mitral until 4 weeks of age when opposing expression patterns are observed.

4. Conclusions

In conclusion, this study has characterized two *Cre*-driver lines and identified age-dependent temporal and spatial specificities in aortic and mitral valve structures. *ScxCre* is best suited for lineage-specific studies in subpopulations of embryonic valve interstitial, but not endothelial cells during stages of remodeling following EMT. As *ScxCre* lines are not inducible, manipulation of this lineage after birth is limited due to the high levels of recombination observed in the embryo. In contrast, *Sox9CreER^{T2}* mice recombine in both VECs and VICs and due to the estrogen response control element, both embryonic and post natal studies can be performed. However, by four weeks of age, expression is low and therefore studies in adult valves may not be informative (Figure 5). Together, these tools have the potential to advance the field by allowing for gene targeting and manipulation in valve cell lineages during embryonic and post natal stages of development, maturation and maintenance.

Figure 3. *Sox9CreER*^{T2} recombination in embryonic heart valve primorida structures. Pregnant *Sox9CreER*^{T2}*:R26*^{GFP} mice were exposed to tamoxifen treatment from E14.5 and harvested at E15.5. (**A**–**D**) Immunohistochemistry to detect GFP expression (Green) following *Sox9CreER*^{T2}*:R26*^{GFP} recombination, and CD31-(Red) positive endothelial cells in aortic (**A**,**B**) and mitral (**C**,**D**) valves at E15.5. (**B**) and (**D**) are high magnification images (40×) of the boxed areas shown in (**A**) and (**C**) at 10×, respectively. Red arrowhead in (**B**) shows the aortic valve annular region. White arrows in **B** and **D** indicate valve interstitial cells, and white arrows, valve endothelial cells. (**E**–**F**) Arrow indicates few GFP-positive cells within the developing myocardium (**E**) and epicardium (**F**). DAPI (blue), indicates nuclei.

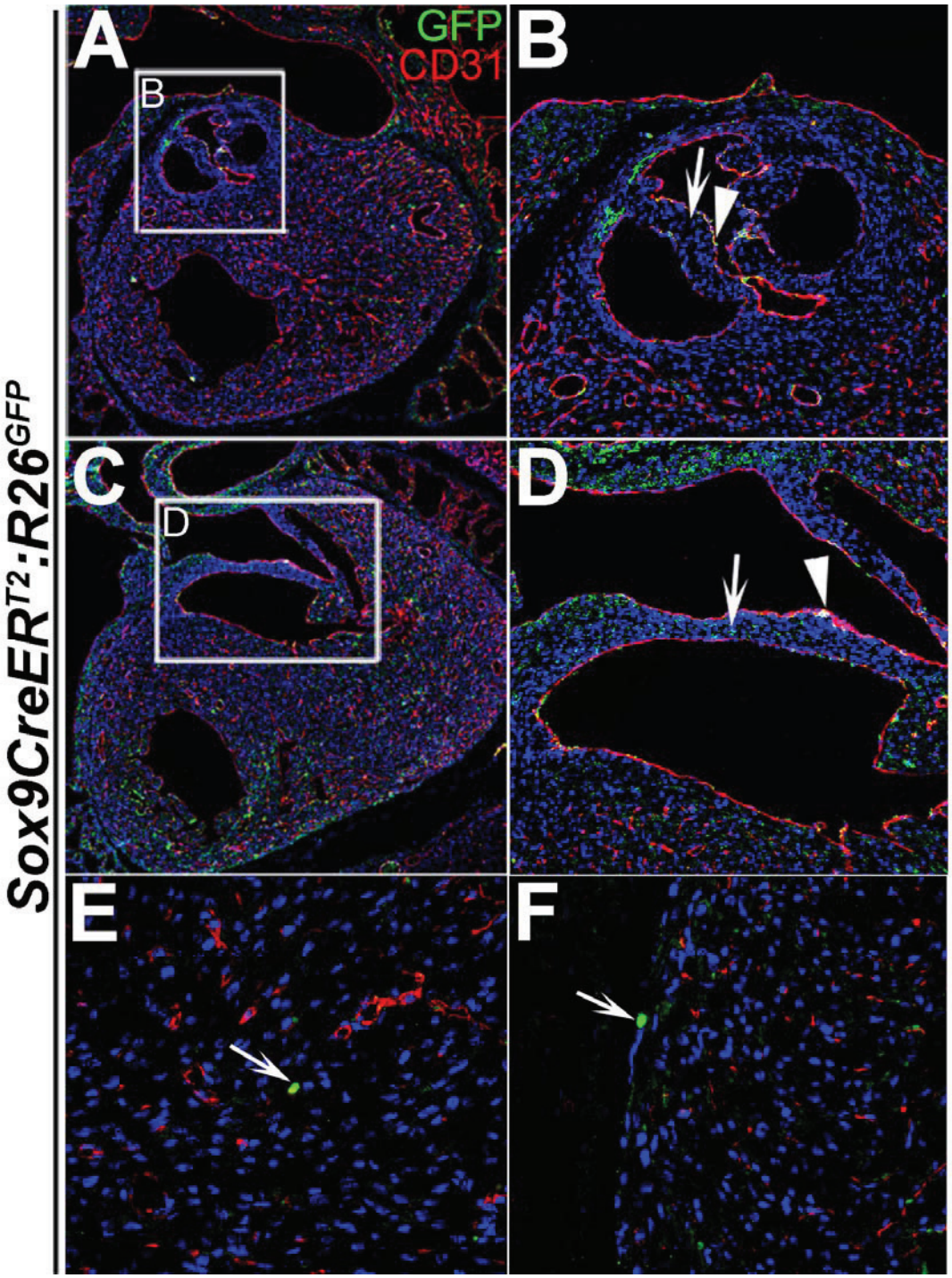

Figure 4. *Sox9CreER*^{T2} recombination in post natal and juvenile heart valve structures. (**A**–**F**) Immunohistochemistry to detect GFP expression (Green) following *Sox9CreER*^{T2}*:R26*^{GFP} recombination and CD31-(Red) positive endothelial cells in aortic (**A**,**B**) and mitral (**C**,**D**) valves from PND12 (**A**,**C**) and 4 week (**B**,**D**) old *Sox9CreER*^{T2}*:R26*^{GFP} mice. Red arrows indicate blood flow direction. White concave arrows indicate valve interstitial cells, and white arrows, valve endothelial cells. (**E**–**F**) Immunohistochemistry of GFP and CD31 in mitral valves from (**E**) tamoxifen-treated *Sox9CreER*$^{T2-}$*:R26*^{GFP} (*Cre* negative) or (**F**) corn oil treated *Sox9CreER*$^{T2-}$*:R26*^{GFP} (*Cre* positive) mice at PND12 to detect non-specific *Cre* recombination (Green). DAPI (blue), indicates nuclei.

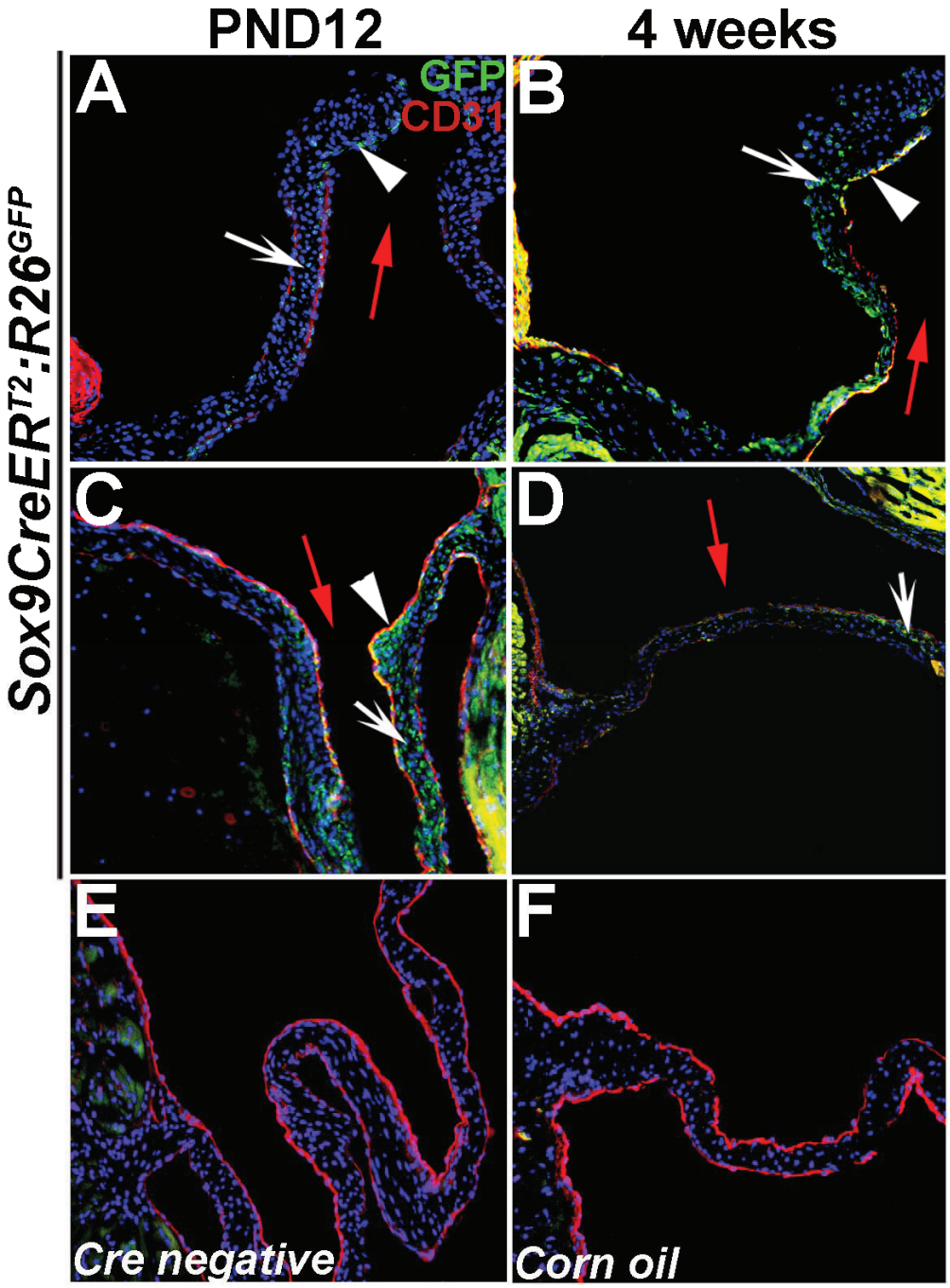

Figure 5. Schematic diagram to review *ScxCre* and *Sox9CreER*^{T2} expression in PND12 (left) and 4 week old (right) aortic (top) and mitral (bottom) heart valves.

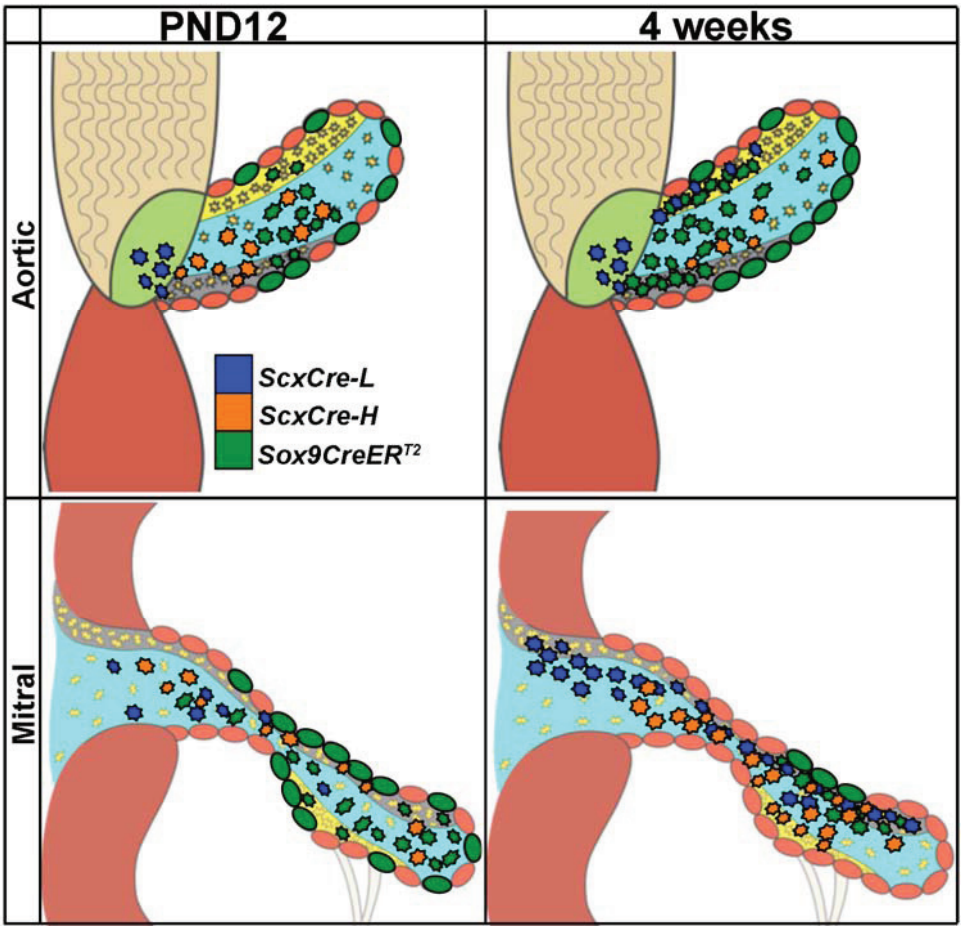

Acknowledgements

We thank Cynthia McAllister and Danielle Huk for technical assistance. This work was supported by American Heart Association Grant in Aid (14GRNT19630003, JL) and Nationwide Children's Hospital Research Institute.

Author Contributions

Blair F. Austin Generated data and captured images; Yuki Yoshimoto Generated ScxCre mouse lines; Chisa Shukunami Generated ScxCre mouse lines; Joy Lincoln Oversaw data generation and prepared the manuscript.

Conflicts of Interest

The authors declare no conflict of interest.

References

1. Tao, G.; Kotick, J.D.; Lincoln, J. Heart valve development, maintenance, and disease: The role of endothelial cells. *Curr. Top. Dev. Biol.* **2012**, *100*, 203–232.

2. Hinton, R.B., Jr.; Lincoln, J.; Deutsch, G.H.; Osinska, H.; Manning, P.B.; Benson, D.W.; Yutzey, K.E. Extracellular matrix remodeling and organization in developing and diseased aortic valves. *Circ. Res.* **2006**, *98*, 1431–1438.
3. Schoen, F.J. Evolving concepts of cardiac valve dynamics: The continuum of development, functional structure, pathobiology, and tissue engineering. *Circulation* **2008**, *118*, 1864–1880.
4. Bosse, K.; Hans, C.P.; Zhao, N.; Koenig, S.N.; Huang, N.; Guggilam, A.; LaHaye, S.; Tao, G.; Lucchesi, P.A.; Lincoln, J.; *et al.* Endothelial nitric oxide signaling regulates Notch1 in aortic valve disease. *J. Mol. Cell. Cardiol.* **2013**, *60*, 27–35.
5. Gould, S.T.; Matherly, E.E.; Smith, J.N.; Heistad, D.D.; Anseth, K.S. The role of valvular endothelial cell paracrine signaling and matrix elasticity on valvular interstitial cell activation. *Biomaterials* **2014**, *35*, 3596–3606.
6. Richards, J.; El-Hamamsy, I.; Chen, S.; Sarang, Z.; Sarathchandra, P.; Yacoub, M.H.; Chester, A.H.; Butcher, J.T. Side-specific endothelial-dependent regulation of aortic valve calcification: Interplay of hemodynamics and nitric oxide signaling. *Am. J. Pathol.* **2013**, *182*, 1922–1931.
7. Walker, G.A.; Masters, K.S.; Shah, D.N.; Anseth, K.S.; Leinwand, L.A. Valvular myofibroblast activation by transforming growth factor-beta: Implications for pathological extracellular matrix remodeling in heart valve disease. *Circ. Res.* **2004**, *95*, 253–260.
8. Lincoln, J.; Alfieri, C.M.; Yutzey, K.E. Development of heart valve leaflets and supporting apparatus in chicken and mouse embryos. *Dev. Dyn.* **2004**, *230*, 239–250.
9. De Lange, F.J.; Moorman, A.F.M.; Anderson, R.H.; Männer, J.; Soufan, A.T.; Vries, C.D.; Schneider, M.D.; Webb, S.; van den Hoff, M.J.B.; Christoffels, V.M. Lineage and morphogenetic analysis of the cardiac valves. *Circ. Res.* **2004**, *95*, 645–654.
10. Lincoln, J.; Garg, V. Etiology of Valvular Heart Disease. *Circ. J.* **2014**, *78*, 1801–1807.
11. Soriano, P. Generalized lacZ expression with the ROSA26 Cre reporter strain. *Nat. Genet.* **1999**, *21*, 70–71.
12. Kisanuki, Y.Y.; Hammer, R.E.; Miyazaki, J.; Williams, S.C.; Richardson, J.A.; Yanagisawa, M. Tie2-Cre transgenic mice: A new model for endothelial cell-lineage analysis *in vivo*. *Dev. Biol.* **2001**, *230*, 230–242.
13. Forde, A.; Constien, R.; Grone, H.J.; Hammerling, G.; Arnold, B. Temporal Cre-mediated recombination exclusively in endothelial cells using Tie2 regulatory elements. *Genesis* **2002**, *33*, 191–197.
14. Robson, A.; Allinson, K.R.; Anderson, R.H.; Henderson, D.J.; Arthur, H.M. The TGFbeta type II receptor plays a critical role in the endothelial cells during cardiac development. *Dev. Dyn.* **2010**, *239*, 2435–2442.
15. Zhou, B.; Wu, B.; Tompkins, K.L.; Boyer, K.L.; Grindley, J.C.; Baldwin, H.S. Characterization of Nfatc1 regulation identifies an enhancer required for gene expression that is specific to pro-valve endocardial cells in the developing heart. *Development* **2005**, *132*, 1137–1146.
16. Wu, B.; Wang, Y.; Lui, W.; Langworthy, M.; Tompkins, K.L.; Hatzopoulos, A.K.; Baldwin, H.S.; Zhou, B. Nfatc1 coordinates valve endocardial cell lineage development required for heart valve formation. *Circ. Res.* **2011**, *109*, 183–192.
17. Jiang, X.; Rowitch, D.H.; Soriano, P.; McMahon, A.P.; Sucov, H.M. Fate of the mammalian cardiac neural crest. *Development* **2000**, *127*, 1607–1616.

18. Nakamura, T.; Colbert, M.C.; Robbins, J. Neural crest cells retain multipotential characteristics in the developing valves and label the cardiac conduction system. *Circ. Res.* **2006**, *98*, 1547–1554.
19. Verzi, M.P.; McCulley, D.J.; de Val, S.; Dodou, E.; Black, B.L. The right ventricle, outflow tract, and ventricular septum comprise a restricted expression domain within the secondary/anterior heart field. *Dev. Biol.* **2005**, *287*, 134–145.
20. Heidt, A.B.; Black, B.L. Transgenic mice that express Cre recombinase under control of a skeletal muscle-specific promoter from mef2c. *Genesis* **2005**, *42*, 28–32.
21. Wessels, A.; van den Hoff, M.J.B.; Adamo, R.F.; Phelps, A.L.; Lockhart, M.M.; Sauls, K.; Briggs, L.E.; Norris, R.A.; van Wijk, B.; Perez-Pomares, J.M.; *et al.* Epicardially derived fibroblasts preferentially contribute to the parietal leaflets of the atrioventricular valves in the murine heart. *Dev. Biol.* **2012**, *366*, 111–124.
22. Lockhart, M.M.; Phelps, A.L.; van den Hoff, M.J.; Wessels, A. The Epicardium and the Development of the Atrioventricular Junction in the Murine Heart. *J. Dev. Biol.* **2014**, *2*, 1–17.
23. Del Monte, G.; Casanova, J.C.; Guadix, J.A.; MacGrogan, D.; Burch, J.B.E.; Pérez-Pomares, J.M.; de la Pompa, J.L. Differential Notch signaling in the epicardium is required for cardiac inflow development and coronary vessel morphogenesis. *Circ. Res.* **2011**, *108*, 824–836.
24. Ovchinnikov, D.A.; Deng, J.M.; Ogunrinu, G.; Behringer, R.R. Col2a1-directed expression of Cre recombinase in differentiating chondrocytes in transgenic mice. *Genesis* **2000**, *26*, 145–146.
25. Lincoln, J.; Kist, R.; Scherer, G.; Yutzey, K.E. Sox9 is required for precursor cell expansion and extracellular matrix organization during mouse heart valve development. *Dev. Biol.* **2007**, *305*, 120–132.
26. Snider, P.; Tang, S.; Lin, G.; Wang, J.; Conway, S.J. Generation of Smad7(-Cre) recombinase mice: A useful tool for the study of epithelial-mesenchymal transformation within the embryonic heart. *Genesis* **2009**, *47*, 469–475.
27. Lindsley, A.; Snider, P.; Zhou, H.; Rogers, R.; Wang, J.; Olaopa, M.; Kruzynska-Frejtag, A.; Koushik, S.V.; Lilly, B.; Burch, J.B.E.; *et al.* Identification and characterization of a novel Schwann and outflow tract endocardial cushion lineage-restricted periostin enhancer. *Dev. Biol.* **2007**, *307*, 340–355.
28. Takeda, N.; Manabe, I.; Uchino, Y.; Eguchi, K.; Matsumoto, S.; Nishimura, S.; Shindo, T.; Sano, M.; Otsu, K.; Snider, P. Cardiac fibroblasts are essential for the adaptive response of the murine heart to pressure overload. *J. Clin. Inv.* **2010**, *120*, 254–265.
29. VanDusen, N.J.; Vincentz, J.W.; Firulli, B.A.; Howard, M.J.; Rubart, M.; Firulli, A.B. Loss of Hand2 in a population of Periostin lineage cells results in pronounced bradycardia and neonatal death. *Dev. Bio.* **2014**, *388*, 149–158.
30. Peacock, J.D.; Levay, A.K.; Gillaspie, D.B.; Tao, G.; Lincoln, J. Reduced sox9 function promotes heart valve calcification phenotypes *in vivo*. *Circ. Res.* **2010**, *106*, 712–719.
31. Levay, A.K.; Peacock, J.D.; Lu, Y.; Koch, M.; Hinton, R.B., Jr.; Kadler, K.E.; Lincoln, J. Scleraxis is required for cell lineage differentiation and extracellular matrix remodeling during murine heart valve formation *in vivo*. *Circ. Res.* **2008**, *103*, 948–956.
32. Sugimoto, Y.; Takimoto, A.; Hiraki, Y.; Shukunami, C. Generation and characterization of ScxCre transgenic mice. *Genesis* **2013**, *51*, 275–283.

33. Murchison, N.D.; Price, B.A.; Conner, D.A.; Keene, D.R.; Olson, E.N.; Tabin, C.J.; Schweitzer, R. Regulation of tendon differentiation by scleraxis distinguishes force-transmitting tendons from muscle-anchoring tendons. *Development* **2007**, *134*, 2697–2708.
34. Sugimoto, Y.; Takimoto, A.; Akiyama, H.; Kist, R.; Scherer, G.; Nakamura, T.; Hiraki, Y.; Shukunami, C. Scx+/Sox9+ progenitors contribute to the establishment of the junction between cartilage and tendon/ligament. *Development* **2013**, *140*, 2280–2288.
35. Pryce, B.A.; Brent, A.E.; Murchison, N.D.; Tabin, C.J.; Schweitzer, R. Generation of transgenic tendon reporters, ScxGFP and ScxAP, using regulatory elements of the scleraxis gene. *Dev. Dyn.* **2007**, *236*, 1677–1682.
36. Kopp, J.L.; Dubois, C.L.; Schaffer, A.E.; Hao, E.; Shih, H.P.; Seymour, P.A.; Ma, J.; Sander, M. Sox9+ ductal cells are multipotent progenitors throughout development but do not produce new endocrine cells in the normal or injured adult pancreas. *Development* **2011**, *138*, 653–665.
37. Murao, H.; Yamamoto, K.; Matsuda, S.; Akiyama, H. Periosteal cells are a major source of soft callus in bone fracture. *J. Bone Miner. Metab.* **2013**, *31*, 390–398.
38. Mao, X.; Fujiwara, Y.; Chapdelaine, A.; Yang, H.; Orkin, S.H. Activation of EGFP expression by Cre-mediated excision in a new ROSA26 reporter mouse strain. *Blood* **2001**, *97*, 324–326.
39. Barnette, D.N.; VandeKopple, M.; Wu, Y.; Willoughby, D.A.; Lincoln, J. RNA-seq analysis to identify novel roles of scleraxis during embryonic mouse heart valve remodeling. *PLoS One* **2014**, *9*, e101425.
40. Espira, L.; Lamoureux, L.; Jones, S.C.; Gerard, R.D.; Dixon, I.M.; Czubryt, M.P. The basic helix-loop-helix transcription factor scleraxis regulates fibroblast collagen synthesis. *J. Mol. Cell. Cardiol.* **2009**, *47*, 188–195.
41. Barnette, D.N.; Hulin, A.; Ahmed, A.S.; Colige, A.C.; Azhar, M.; Lincoln, J. Tgfbeta-Smad and MAPK signaling mediate scleraxis and proteoglycan expression in heart valves. *J. Mol. Cell. Cardiol.* **2013**, *65*, 137–146.
42. Bagchi, R.A.; Czubryt, M.P. Synergistic roles of scleraxis and Smads in the regulation of collagen 1alpha2 gene expression. *Biochim. Biophys. Acta* **2012**, *1823*, 1936–1944.
43. Peacock, J.D.; Huk, D.J.; Ediriweera, H.N.; Lincoln, J. Sox9 transcriptionally represses Spp1 to prevent matrix mineralization in maturing heart valves and chondrocytes. *PLoS One* **2011**, *6*, e26769.